University of Tehran Press

Online ISSN: 2345-475X

DESERT

Home page: https://jdesert.ut.ac.ir/

Integrated Assessment of Drought and Vegetation Dynamics in an Arid Region of Southwest Iran

Amir Khazaei[1*], Fatemeh Sahragard[2], Elham Yousefi[2]

[1] Department of Water Science and Engineering, Faculty of Agriculture, University of Birjand, Birjand, Iran. Email: amir.khazaei@birjand.ac.ir

[2] Department of Environment, Faculty of Natural Resources and Environment, University of Birjand, Birjand, Iran.

Article Info.

Article type:
Research Article

Article history:
Received: 09 Nov. 2025
Received in revised from: 29 Mar. 2026
Accepted: 02 Apr. 2026
Published online: 09 Apr. 2026

Keywords:
Drought,
Vegetation Health Index,
MODIS,
Khuzestan,
Remote Sensing,
Google Earth Engine.

ABSTRACT

Drought, a pervasive natural hazard, poses serious threats to ecosystems, agriculture, and water resources, particularly in arid and semi-arid regions. This study provides a comprehensive long-term assessment of drought dynamics, vegetation health, and hydrological variations in Khuzestan Province, southwest Iran, during 2000–2023. Meteorological drought was carefully quantified using the Standardized Precipitation Index (SPI), while vegetation stress and temperature impacts were evaluated through the Vegetation Condition Index (VCI), Temperature Condition Index (TCI), and the integrated Vegetation Health Index (VHI) derived from MODIS satellite data processed in Google Earth Engine. Results revealed pronounced seasonal and interannual variability, with severe and recurrent summer droughts accompanied by occasional wet anomalies. Central and northern areas experienced the highest vegetation stress, whereas southern regions remained relatively stable and resilient throughout the study period. Hydrological analyses using GRACE and SMAP datasets indicated persistent and significant reductions in terrestrial water storage and soil moisture, strongly correlated with vegetation health indicators. Correlation analysis demonstrated that VHI was primarily influenced by VCI, with SPI and TCI exerting secondary but notable effects. Overall, the findings emphasize the crucial value of multi-index, satellite-based monitoring for understanding drought–vegetation interactions, improving early-warning capabilities, and supporting sustainable water, ecosystem, and agricultural management in semi-arid environments.

Cite this article: Khazaei, A., Sahragard, F., Yousefi, E. (2026). Integrated Assessment of Drought and Vegetation Dynamics in an Arid Region of Southwest Iran. DESERT, 30 (2), DOI: 10.22059/jdesert.2025.107091

DOI: 10.22059/jdesert.2025.107091

Publisher: University of Tehran Press

1. Introduction

Drought, recognized as a creeping and pervasive natural hazard, poses serious threats to ecosystems, agricultural productivity, and the sustainability of water resources. Its impacts are particularly severe in arid and semi-arid regions, where water scarcity is already a defining characteristic (Bahrami *et al*., 2019, 2021; Kogan and Kogan, 2019; Narayan *et al*., 2024; Khalili *et al*., 2024). The increasing frequency and intensity of drought events, intensified by ongoing climate change, highlight the urgent need for effective monitoring and mitigation strategies to safeguard vulnerable communities and ecosystems (Remer *et al*., 2024; Rahimi *et al*., 2025b).

Drought is commonly classified into four categories: meteorological, agricultural, hydrological, and socio-economic. Meteorological drought arises from prolonged precipitation deficits, agricultural drought manifests in reduced crop yields and vegetation stress, hydrological drought is associated with declining surface and groundwater availability, and socio-economic drought emerges through disruptions to food security, livelihoods, and human well-being (Souza *et al*., 2021; Qin *et al*., 2021; Sharifi *et al*., 2022). These overlapping dimensions emphasize the complexity of drought as both an environmental and socio-economic phenomenon.

Traditional drought monitoring has largely relied on ground-based meteorological data, which, despite their importance, are constrained by sparse spatial coverage and high operational costs (Heim, 2002; Amini and Hatamzadeh, 2023). Advances in remote sensing provide powerful alternatives, enabling spatially and temporally extensive monitoring through satellite-derived indices such as the Normalized Difference Vegetation Index (NDVI) and Land Surface Temperature (LST) (Javed *et al*., 2021). In particular, indices like the Vegetation Condition Index (VCI), Temperature Condition Index (TCI), Vegetation Health Index (VHI), and the Standardized Precipitation Index (SPI) have proven valuable for assessing vegetation stress, climatic variability, and drought dynamics across diverse environments (Singh *et al*., 2003; Gidey *et al*., 2018; Bento *et al*., 2018; Hang *et al*., 2024; Osmani *et al*., 2024; Quiring and Ganesh, 2010; Rezaeimoghadam *et al*., 2013).

Traditional ground-based assessments are limited by sparse coverage and high costs (Heim, 2002; Amini and Hatamzadeh, 2023). Remote sensing offers extensive spatial and temporal coverage, enabling effective drought monitoring (Bhuiyan *et al*., 2006; Kogan, 1990). Key indices include NDVI, LST, VCI, TCI, and VHI for assessing vegetation stress, while SPI provides precipitation-based drought analysis (Javed *et al*., 2021; Singh *et al*., 2003; Gidey *et al*., 2018; Bento *et al*., 2018; Hang *et al*., 2024; Osmani *et al*., 2024; Quiring and Ganesh, 2010; Rezaeimoghadam *et al*., 2013).

Studies conducted in Iran have widely used remote sensing and meteorological indices to assess drought. Siasar *et al*. (2025) used MODIS-based VCI, TCI, VHI, SVI, and SPI in Sistan and Baluchestan and identified severe drought events in multiple years, showing strong correlation between indices and precipitation. Ghobadi *et al*. (2025) applied NDVI, VCI, TCI, and VHI in Lorestan, Iran, revealing increased drought severity and reduced drought-free areas over two decades. Rahnama *et al*. (2022) used Landsat-based NDVI, SAVI, and SR with SPI in Birjand, Shiraz, and Rasht, showing strong agreement between satellite and meteorological data. Shekaryan *et al*. (2022) reported severe droughts in southern North Khorasan over a 19-year period. Kouhestani Eyndin *et al*. (2022) examined socioeconomic factors affecting farmers' vulnerability to drought in Dorood Faraman. Rashtabari *et al*. (2021) identified SVI as the most effective MODIS-based drought index in the Zayandehroud Basin. Dehghan *et al*.

(2017) projected increased drought frequency in Fars Province using Palmer Drought Severity Index. Saadian *et al*. (2021) mapped land use changes in the Karkheh Basin using GEE, confirming NDVI's effectiveness. Karimi *et al*. (2019) and Soleimani *et al*. (2019) highlighted the value of NDVI, VCI, and VHI for monitoring agricultural drought.

International studies have also confirmed the usefulness of remote sensing and Google Earth Engine. Rousta *et al*. (2025) analyzed meteorological and agricultural droughts using VCI, TCI, and VHI, highlighting their effectiveness in arid and semi-arid regions. Alzurqani *et al*. (2024) developed a GEE-based application combining VCI and TCI into VHI for efficient drought monitoring in various regions.. Lazrqani *et al*. (2024) found that 32% of Arkansas, USA, experienced multiple drought classes. Thanh *et al*. (2024) predicted drought stress under climate change in the Southern Central Highlands of Vietnam. Their study highlighted increasing drought frequency and its impacts on water resources and socio-economic development in the region, showing the usefulness of remote sensing and modeling approaches for drought assessment. Taheri Ghazvini and Carrion (2023) applied VCI, TCI, and SPI in GEE across Iran to monitor drought. Ramla Khan and Gilani (2021) used NDVI in GEE to study agricultural drought in Asia, Africa, and Australia. Jantakut (2021) monitored urban tree drought stress in Thailand with SVI. Aksoy *et al*. (2019) and Winkler *et al*. (2017) demonstrated long-term drought monitoring using VHI, VCI, and SPI in Turkey and Africa.

While numerous studies have demonstrated the effectiveness of remote sensing and meteorological data for drought monitoring, significant gaps remain in long-term, integrated assessments that combine multiple indices to fully capture drought dynamics. In regions like Khuzestan, which are highly vulnerable to prolonged agricultural and meteorological droughts, most prior research has focused on individual indices or short-term analyses, failing to reveal the complex interactions among vegetation health, temperature stress, and precipitation deficits.

The study covers the period 2000–2023. Due to data availability constraints, GRACE satellite data were used to analyze groundwater storage variations for the period 2002–2017, while SMAP soil moisture products were available for 2015–2020. In contrast, meteorological and vegetation-based drought indices, including SPI, VCI, TCI, and VHI, were calculated consistently for the full 2000–2023 period.

2. Materials and methods

2.1 study area

The study area encompasses Khuzestan Province in southwestern Iran, bordered by Ilam, Lorestan, Chaharmahal and Bakhtiari, Kohgiluyeh and Boyer-Ahmad to the north and east, and Bushehr Province to the south. Covering approximately 63,622 km² with an estimated population of 4.7 million, Khuzestan is morphotectonically divided into the folded and unfolded Zagros units, resulting in a predominantly mountainous northern region and a lowland southern plain, with considerable elevation differences between these zones (Figure 1; Negahban *et al*., 2024; Ganjavian *et al*.,2021).

Hydrologically, major rivers such as the Karun, Karkheh, and Dez discharge into the Khuzestan plain, making it one of the most critical and water-sensitive catchments in southwestern Iran. The climate is mainly semi-arid to arid, with average annual precipitation ranging from 144 to 254 mm. The combination of significant water resources, climatic variability, recurrent droughts, and unsustainable water extraction exerts substantial environmental pressure, posing serious challenges to ecosystems and agricultural activities in the province (Piri & Ansari Ghojghar, 2025).

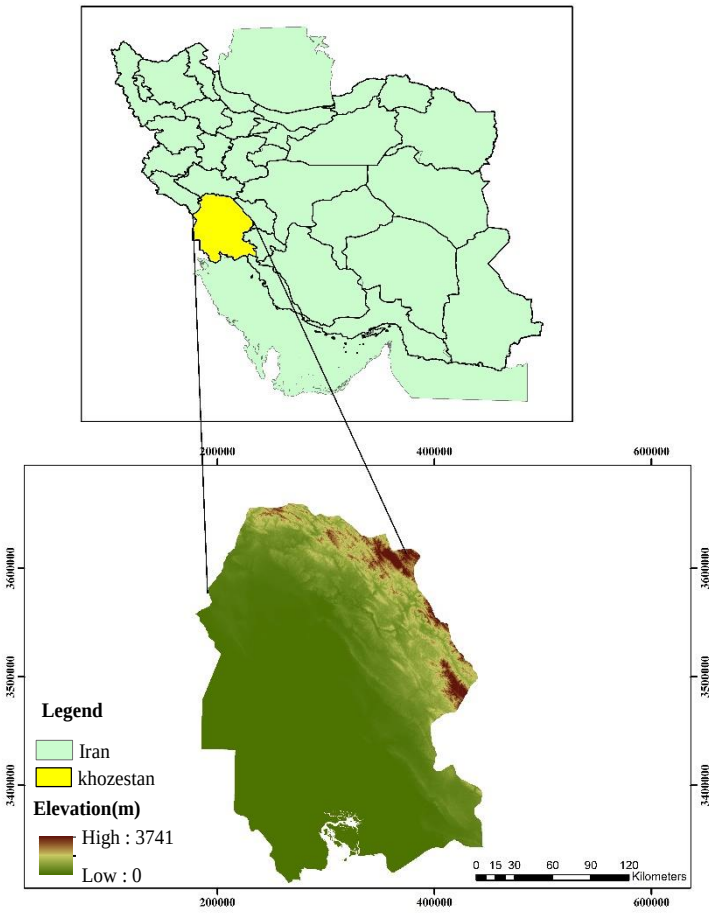

Figure 1. Map showing Khuzestan Province and its position within Iran

2.2 Meteorological Drought Indices

The overall study period spans from 2000 to 2023; however, the temporal coverage of the employed datasets varies depending on sensor availability. Meteorological and vegetation-based drought indices, including the SPI, VCI, TCI and VHI, were derived for the entire 2000–2023 period to characterize long-term drought and vegetation dynamics. Groundwater storage variations were assessed using GRACE satellite data, which are available from 2002 to 2017, corresponding to the operational lifetime of the original GRACE mission. In addition, surface and subsurface soil moisture conditions were analyzed using SMAP data, which cover the period from 2015 to 2020. These datasets were analyzed within their respective valid temporal ranges and interpreted in an integrated framework while accounting for their temporal limitations.

Monthly precipitation data for the study period (2000–2023) were primarily obtained from the CHIRPS dataset (5 km spatial resolution) due to its complete spatial coverage and temporal consistency. Observational rainfall records from the Iranian Meteorological Organization (IRIMO) were used to validate and assess the quality of the CHIRPS data at selected stations. No direct merging of CHIRPS and IRIMO datasets was performed; IRIMO records served

solely for validation purposes.

To ensure consistency among multi-source satellite datasets with different spatial and temporal resolutions, all variables were harmonized prior to analysis. MODIS-based vegetation and temperature indices (8-day) and SMAP soil moisture data (3-day) were aggregated to monthly values using mean compositing to match the native temporal resolution of GRACE data.

Given the coarse effective resolution of GRACE, spatial harmonization was performed at the regional scale. Indices were first calculated at their original resolutions and then spatially averaged over Khuzestan Province to generate area-mean time series. This approach avoids uncertainties associated with direct spatial resampling and allows physically meaningful comparisons among datasets. GRACE and SMAP data were integrated within a drought-propagation framework, in which SMAP represents short-term soil moisture variability, while GRACE reflects long-term cumulative water storage changes. These datasets were therefore interpreted as complementary indicators rather than directly equivalent variables, enabling an integrated assessment of drought dynamics while accounting for their functional differences.

Standardized Precipitation Index (SPI)

the study area. SPI quantifies drought severity based on precipitation anomalies relative to the long-term historical record. Its calculation requires monthly precipitation data, which can be analyzed over multiple time scales (e.g., 1, 3, 6, 12 months), allowing detection of both short-term and long-term droughts.

In this study, SPI was calculated at 1-, 3-, 6-, 9-, 12-, 24-, and 48-month timescales using long-term monthly precipitation data. The accumulated precipitation for each time window was fitted to a Gamma probability distribution, which is widely recommended for SPI computation. The shape and scale parameters of the Gamma distribution were estimated using the maximum likelihood method. The cumulative probability of the observed precipitation was then transformed into a standard normal variable, yielding the SPI value for each month. Positive SPI values indicate wetter-than-average conditions, whereas negative values indicate drier-than-average conditions. The standard SPI classification used in this study is presented in Table 1.

Table 1. Standard SPI Classification (Ranking)

SPI Value	Category (Rank)	Condition
SPI ≥ +2.0	Extremely Wet	Very Severe Wet Spell
+1.5 to +1.99	Severely Wet	Severe Wet Spell
+1.0 to +1.49	Moderately Wet	Moderate Wet Spell
−0.99 to +0.99	Near Normal	Normal Conditions
−1.0 to −1.49	Moderately Dry	Moderate Drought
−1.5 to −1.99	Severely Dry	Severe Drought
SPI ≤ −2.0	Extremely Dry	Very Severe Drought

2.3 Vegetation Indices

Vegetation Condition Index

The VCI was originally developed by Huete (1996). This index represents the vegetation status of a region and is calculated as a function of the minimum and maximum NDVI values over a multi-year period. VCI also provides a quantitative estimation of the climatic effects on

vegetation. During periods of drought stress, NDVI values decrease, indicating a decline in vegetation health. However, a single NDVI image only reflects the relative health of vegetation at a specific point in time, whereas VCI captures vegetation dynamics over a time series. This index reduces the impact of seasonal noise through normalization. The VCI is computed using Equation (1).

$$VCI_i = \frac{NDVI - NDVI_{min}}{NDVI_{max} - NDVI_{min}} \times 100 \quad (1)$$

where VCI_i is the NDVI value for a specific month, and NDVImax NDVImin and are the maximum and minimum NDVI values for that month over the study period. VCI ranges from 0 to 100, with values near 0 indicating poor vegetation conditions and severe drought, and values close to 100 representing favorable vegetation conditions.

Temperature Condition Index

The TCI, introduced by Kogan (1995), is based on the principle that land surface or canopy temperature increases under water stress conditions due to reduced vegetation cover and soil moisture. Since the occurrence and development of drought are closely related to LST, this index is widely used to evaluate temperature-related vegetation stress. An increase in LST during the growing season indicates unfavorable conditions or drought, whereas lower LST values reflect healthy conditions. TCI, derived from thermal infrared data, has been widely used for drought monitoring. TCI is calculated using Equation (2):

$$TCI_i = \frac{\mathrm{LST_{max}} - \mathrm{LST}_i}{\mathrm{LST_{max}} - \mathrm{LST_{min}}} \times 100 \quad (2)$$

where TCI_i is the TCI, for a specific month, LST_i is the land surface temperature for that month, and $\mathrm{LST_{max}}$ and $\mathrm{LST_{min}}$ are the maximum and minimum LST values for the corresponding month over the study period. The index ranges from 0 to 100, with values near 0 indicating severe drought and values close to 100 representing favorable conditions.

Vegetation Health Index

The VHI integrates the TCI, and the VCI, representing the thermal and moisture conditions of vegetation, respectively. By combining temperature- and moisture-related vegetation stress, VHI provides an effective indicator for drought monitoring and the assessment of crop and vegetation health.. VHI was introduced by Kogan in 2001. The index is computed using Equation (3):

$$VHI: (0.5*VCI)+(0.5*TCI) \quad (3)$$

This formulation accounts for vegetation sensitivity to moisture during canopy development and to temperature during the flowering stage, providing an integrated measure of vegetation health.

2.4 Google Earth Engine

All satellite and geospatial data used in this study were processed using the GEE platform (Gorelick *et al*., 2017), which provides cloud-based access to extensive satellite imagery archives, including Landsat and Sentinel data.

2.5 Methodological Framework

1.2.5. Data Acquisition and Preprocessing

Monthly precipitation data were obtained from the Iranian Meteorological Organization (IRIMO). The precipitation records were spatially interpolated using the Inverse Distance Weighting method to produce continuous gridded datasets required for drought index calculations. Remotely sensed products from the MODIS Terra platform, including MOD13A2 NDVI and MOD11A2 LST, were retrieved using GEE and processed to analyze vegetation dynamics and surface temperature conditions. In addition, GRACE satellite data were used to investigate long-term variations in terrestrial water storage anomalies (TWSA), while SMAP data were employed to assess soil moisture variability.

2.2.5 Drought Index Computation

SPI was calculated at a three-month timescale to characterize short- to medium-term meteorological drought conditions. Vegetation-based drought indices, including the VCI, TCI and VHI, were derived from MODIS-based NDVI and LST datasets according to Equations (1–3). To ensure consistency and comparability, all indices were normalized to a uniform scale ranging from 0 to 100.

3.2.5. Temporal and Spatial Analysis

Monthly and annual time series were generated for SPI, VCI, TCI, and VHI to examine seasonal patterns and interannual variability. Spatial distribution maps were produced for each index to identify drought-prone areas and relatively resilient zones across the study region.

4.2.5. Hydrological and Statistical Analysis

Hydrological drought conditions were evaluated using GRACE-derived terrestrial water storage anomalies and SMAP soil moisture data. Pearson correlation coefficients were computed to quantify the relationships among meteorological, vegetation, and hydrological drought indicators, including SPI, VHI, GRACE, and SMAP datasets. Temporal trends were assessed using the non-parametric Mann–Kendall test, and Sen's slope estimator was applied to determine the magnitude and direction of detected trends.

5.2.5. Integration and Interpretation of Drought Conditions

An integrated drought severity map was generated through a weighted overlay approach combining SPI and VHI indices. Comparative analyses were conducted across the northern, central, and southern regions of Khuzestan Province to examine spatial heterogeneity in drought impacts and vegetation response patterns.

This integrative framework links atmospheric, hydrological, and ecological components, providing a comprehensive understanding of drought behavior. The use of GEE ensures computational efficiency, reproducibility, and scalability for long-term regional drought monitoring (Figure 2).

3. Results and discussion

3.1. Analysis of Standardized Precipitation Index (SPI)

The SPI results indicate recurrent drought episodes throughout the study period, reflecting persistent meteorological drought conditions in Khuzestan Province. These findings are consistent with earlier studies conducted in southwestern Iran, which reported frequent negative

SPI values associated with reduced precipitation and prolonged dry spells (Zarei *et al*., 2020; Tabari *et al*., 2013). Moreover, several studies have demonstrated that SPI derived from CHIRPS precipitation data performs comparably to gauge-based observations in detecting drought events, further supporting the robustness of the approach used in this study (Bayissa *et al*., 2018; Nouri *et al*., 2022).

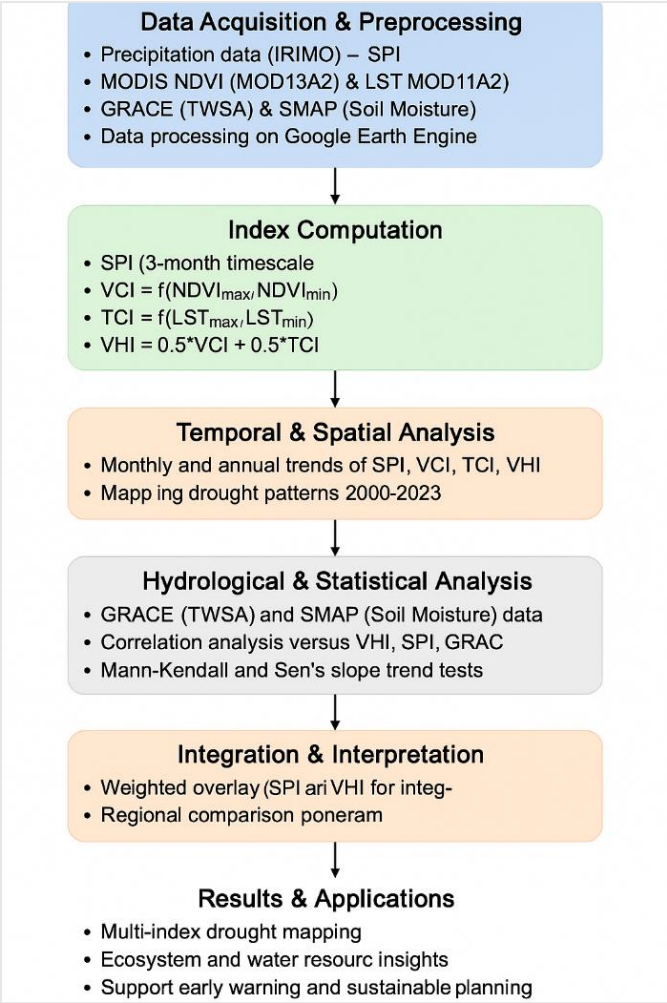

Figure 2. Workflow of the study methodology in Khuzestan Province

The ability of SPI to capture both short-term precipitation anomalies and longer-term drought trends observed in this study aligns with findings reported in other arid and semi-arid regions worldwide (Vicente-Serrano *et al*., 2010). The classification of SPI values and corresponding drought and wet conditions, presented in Table 1, further confirms the effectiveness of SPI as a reliable indicator for monitoring meteorological drought conditions in Khuzestan Province.

Overall, the strong agreement between the SPI patterns identified in this study and those reported in previous regional and global investigations reinforces the validity of combining SPI with high-resolution CHIRPS precipitation data for long-term drought monitoring and climate variability assessment in southwestern Iran.

The SPI time series from 2000 to 2023 reveals substantial seasonal and interannual variability. The early years (2000–2004) were marked by alternating dry and wet periods. For instance, prolonged moderately dry conditions appeared in mid-2000 (April–October, SPI ≈ −0.39 to −0.73), while extreme wet events occurred in December 2000 (SPI = 2.97) and December 2001 (SPI = 5.10), classified as extremely wet.

Between 2005–2010, SPI values fluctuated between approximately −0.73 and 2.42, indicating Near Normal conditions with occasional short-term wet peaks, such as January 2006 (SPI = 2.42) and December 2005 (SPI = 2.05). Dry spells persisted during summer months, especially June–August, reflecting Moderately Dry conditions.

During 2011–2015, the SPI generally remained within the Near Normal range (−0.73 to 1.94), with short extreme wet events, e.g., December 2015 (SPI = 1.94), while dry periods dominated summer months.

From 2016–2020, SPI patterns were mostly Near Normal, punctuated by short-term wet peaks such as December 2016 (SPI = 2.03) and January 2019 (SPI = 2.59), alongside consistent moderately dry periods during summer.

Recent years (2021–2023) exhibit predominantly negative SPI during spring and summer, reflecting Moderately Dry to Severely Dry conditions, e.g., June–August 2021 (SPI ≈ −0.73). Notable wet events occurred in December 2021 (SPI = 2.15) and December 2022 (SPI = 1.06), highlighting short-term Extremely Wet conditions.

Overall, the 2000–2023 SPI record illustrates a pattern of seasonal wet and dry cycles, with extreme wet events being less frequent but highly pronounced, while dry conditions dominate summer months across most years (Figure 3).

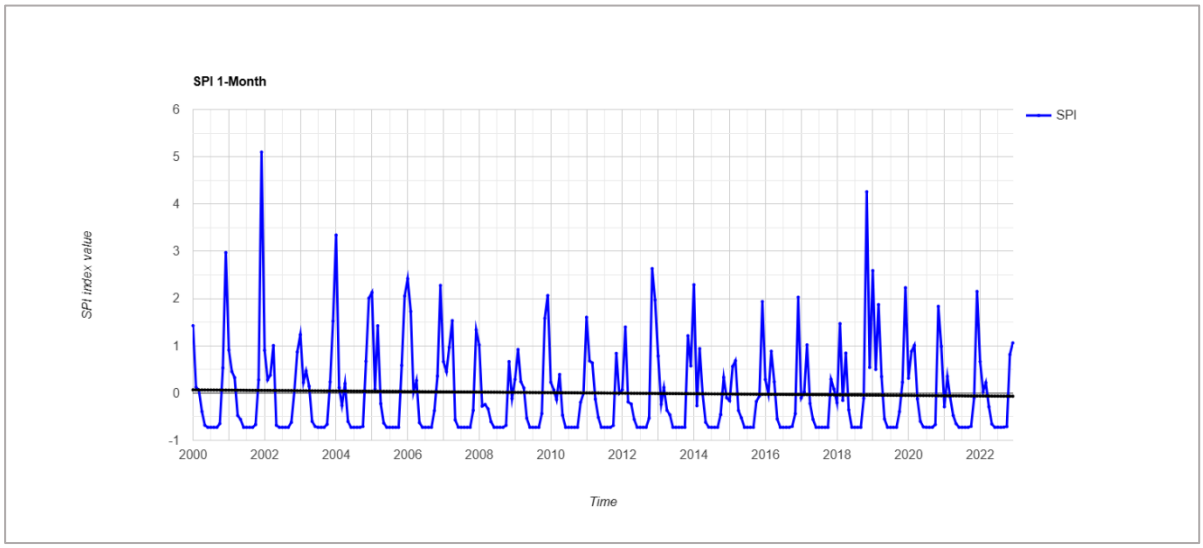

Figure 3. Average Monthly 1-Month SPI in Khuzestan Province, 2000–2023

3.2. Spatial Analysis

The SPI map (Figure 4), ranging from 0.42 to 3.19, indicates the highest SPI values are concentrated in the central and eastern parts of the region, reflecting above-average precipitation and severe wet spells. Western areas show lower SPI values, generally corresponding to near normal or moderately dry conditions. These spatial differences may be

attributed to topography, climate gradients, and convective rainfall patterns.

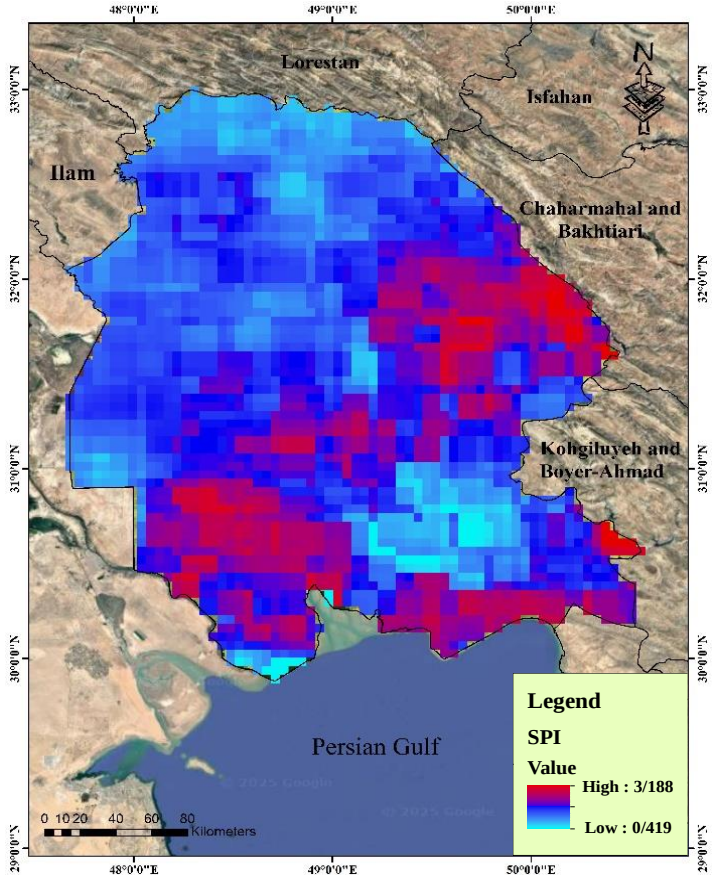

Figure 4. Average Monthly 1-Month SPI in Khuzestan Province, 2000–2023

3.3. Vegetation Condition Index

The VCI values ranged from 0.18 to 0.69, indicating varying vegetation conditions from stressed to optimal states. Lower values (e.g., 2008–2009 and 2011–2012) corresponded to years of significant drought, while higher values (2019–2023) reflected favorable climatic conditions and improved vegetation vigor. Spatially, the highest VCI values (dark blue regions) were concentrated in the southern and southwestern parts of Khuzestan, while lower values (orange to brown areas) dominated the central and northeastern regions, representing zones affected by prolonged dryness.

The temporal pattern of VCI (Figure 5) exhibits distinct seasonal oscillations, characterized by declines during late spring and summer when temperature and evapotranspiration rates are highest—and recoveries during autumn and winter, coinciding with the onset of precipitation and cooler conditions.

A linear regression analysis of the time series revealed a slightly positive trend ($R^2 = 0.41$, $p < 0.05$), suggesting gradual improvement in vegetation health in recent years, potentially linked to improved water resource management, reforestation efforts, and short-term climatic recovery. However, notable periods of vegetation stress—particularly 2007–2009, 2014–2016, and 2021–2022—remain evident, reflecting the persistence of drought episodes in parts of the province.

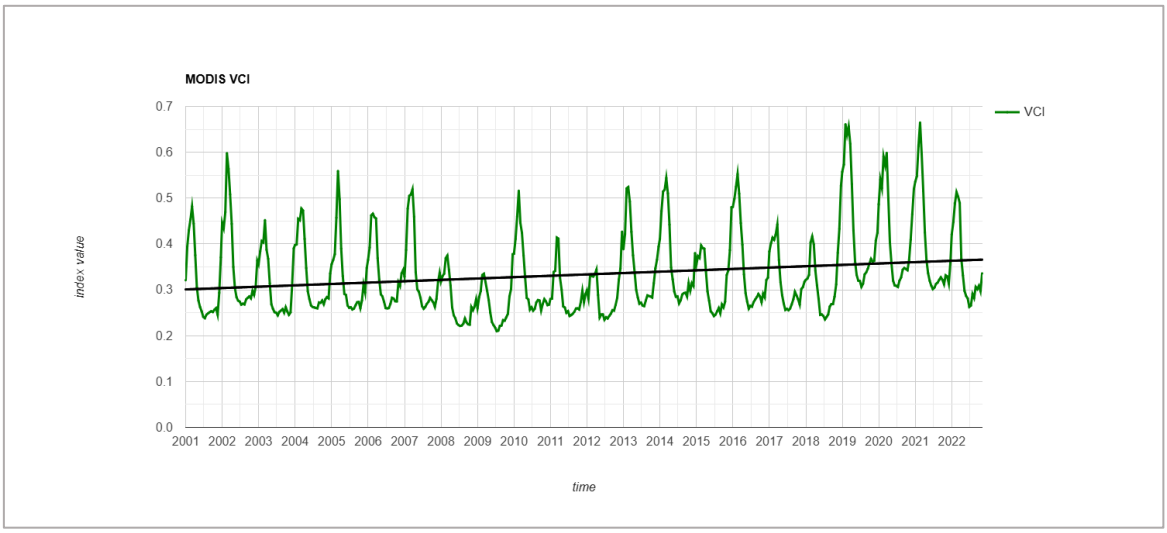

Figure 5. Temporal variations of the VCI in 2000–2023, derived from MODIS NDVI (MOD13Q1) via GEE

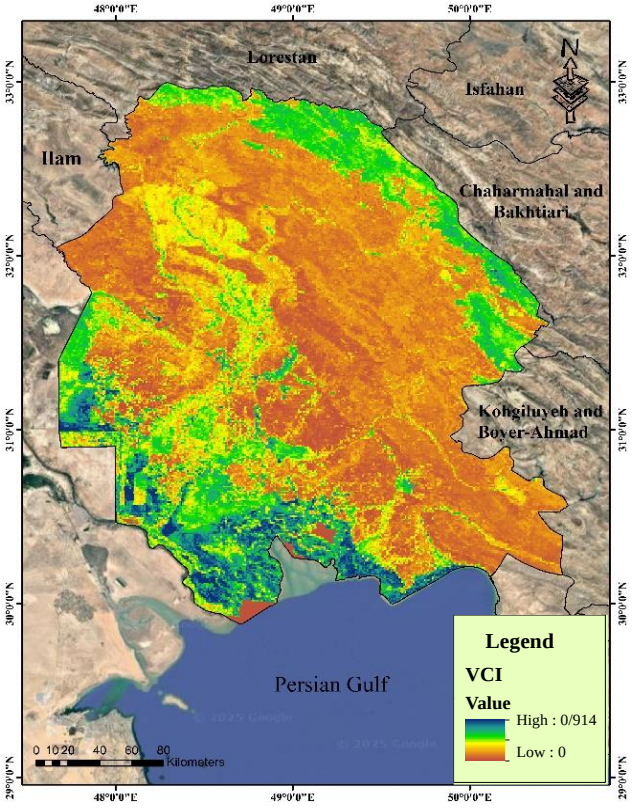

Figure 6. VCI map of Khuzestan Province for (2000-2023).

3.4. Temperature Condition Index

Spatially, TCI values ranged from 0.188 to 0.675, indicating significant variability in vegetation dryness across Khuzestan Province. Higher TCI values correspond to increased

vegetation dryness and thermal stress, while lower values indicate more favorable moisture conditions. As illustrated in Figure 7, the highest TCI values were concentrated in the southern and southwestern regions, which experienced more severe heat stress and lower moisture availability. Conversely, lower TCI values were recorded in the northern and central areas, reflecting cooler and relatively more humid conditions.

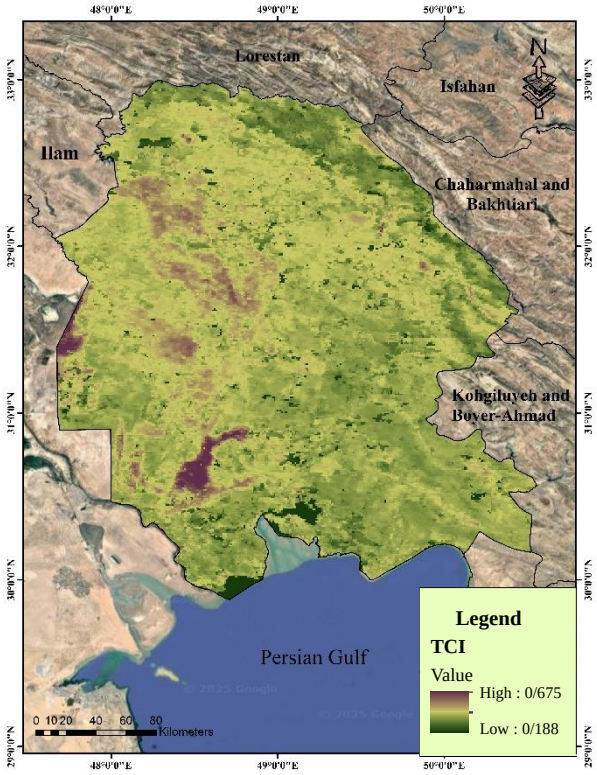

Figure 7. TCI map of Khuzestan Province for (2000-2023).

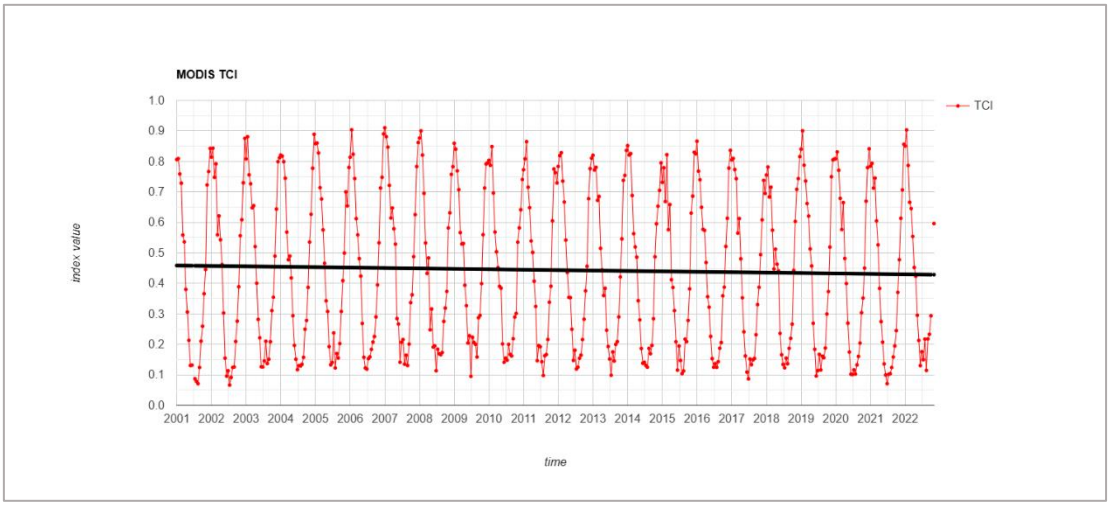

Figure 8. Time-series variations of the TCI extracted from GEE for the period (2000–2023).

The temporal dynamics of TCI (Figure 8) display distinct seasonal fluctuations, with index values peaking during summer months (June–August) when surface temperatures and evapotranspiration rates are highest, leading to intensified vegetation dryness. In contrast, lower TCI values occurred during winter and early spring (December–March), representing improved moisture conditions and reduced thermal stress within the vegetation canopy.

From a long-term perspective, the TCI trend over 2000–2023 indicates a gradual decline in thermal stress, suggesting that plant moisture conditions have slightly improved in recent years. This trend may be attributed to interannual climate variability, improved irrigation management, and regional shifts in precipitation patterns. Nevertheless, several years—particularly 2008–2009, 2014–2016, and 2021–2022—exhibited noticeable spikes in TCI values, corresponding to major regional drought episodes observed in satellite-based vegetation indices.

Overall, the integration of TCI with other indices such as VCI and VHI provides a comprehensive understanding of vegetation health dynamics under varying climatic conditions. The use of GEE not only facilitated large-scale data analysis but also enhanced temporal monitoring accuracy, enabling the detection of both seasonal fluctuations and long-term drought trends across Khuzestan Province.

3.5. Vegetation Health Index

The VHI serves as a comprehensive indicator for assessing vegetation health and drought severity by integrating the VCI and the TCI. VHI was computed using Equation (3). All data processing and analysis were performed within the GEE cloud-based platform, enabling efficient management of large-scale satellite datasets. The study utilized MODIS products, including MOD13A1 (NDVI and EVI) and MOD11A2, with an 8-day temporal resolution covering 2000–2023.

The study area, corresponding to Khuzestan Province, was delineated and all imagery was clipped to its spatial extent. The VCI and TCI, were computed according to Equations (1) and (2), respectively, and temporally synchronized to generate a combined VHI dataset. A time series of 8-day interval images was produced for each index throughout the study period, providing continuous coverage for vegetation and temperature analysis.

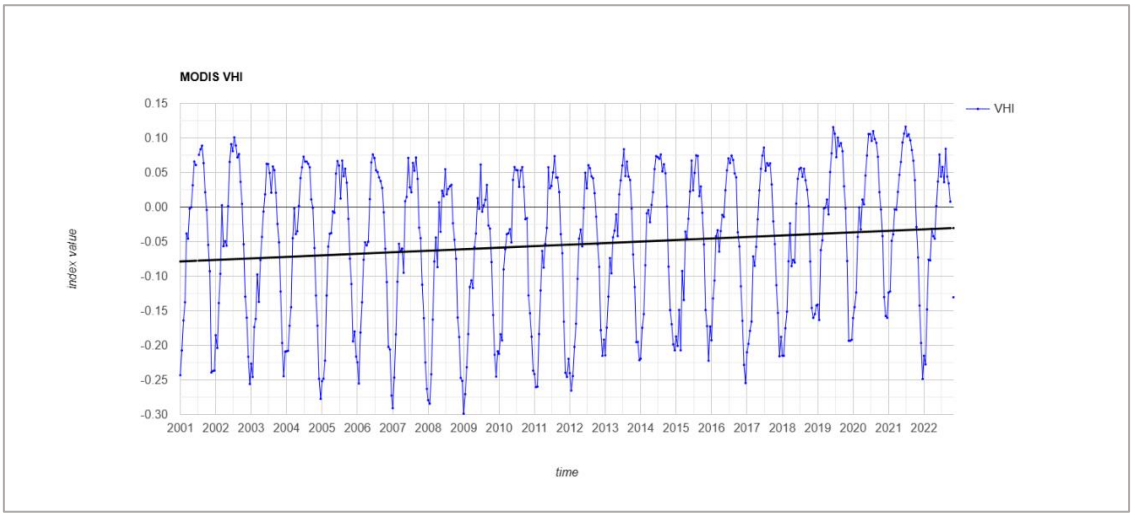

Figure 9. Time-series variations of the VHI derived from GEE for the period (2000–2023).

Temporal analysis of the VHI dataset reveals clear seasonal patterns. Generally, VHI values increase during spring and summer, indicating healthier vegetation and optimal growth conditions, while decreasing during autumn and winter due to drought stress and moisture deficits. For example, in early 2001, VHI values were negative (e.g., –0.243 on January 1, 2001), indicating vegetation stress under low VCI values and high temperatures. Positive VHI values emerged in late spring and summer (e.g., 0.084 on July 28, 2001), reflecting improved vegetation health. Similar seasonal dynamics were observed across subsequent years, with interannual fluctuations influenced by drought events and climatic variability (Figure 9).

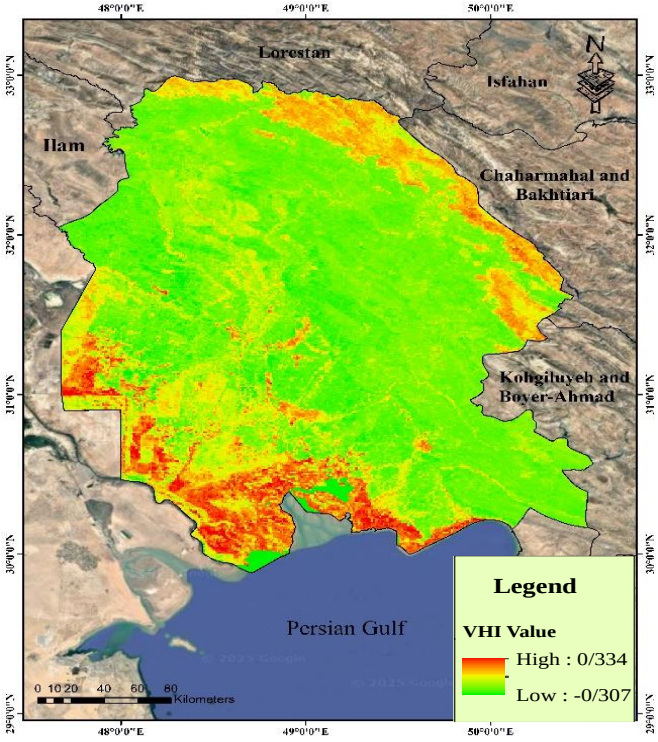

Figure 10. VHI map of Khuzestan Province derived from GEE (2000–2023)

Spatially, the highest VHI values were recorded in the southern and southwestern parts of Khuzestan, reaching up to 0.334, whereas lower values down to –0.307 occurred in drier zones and during drought years. The integrated analysis of VCI, TCI, and VHI over the 2000–2023 period demonstrates both seasonal cycles and long-term trends, providing insights into vegetation resilience, drought impacts, and the effectiveness of water management strategies (Figure 10).

All datasets, maps, and time-series plots were generated and exported from GEE, offering a reproducible framework for long-term drought monitoring, vegetation health assessment, and sustainable land management in Khuzestan Province. The time-series data also enables identification of critical periods of vegetation stress, facilitating targeted interventions for agriculture and natural resource management.

The analysis of TCI, VCI, and VHI from 2000 to 2023provides a comprehensive overview of vegetation health and drought patterns over the 25-year period. Figure 11 presents these indices across time, enabling seasonal and interannual comparisons.

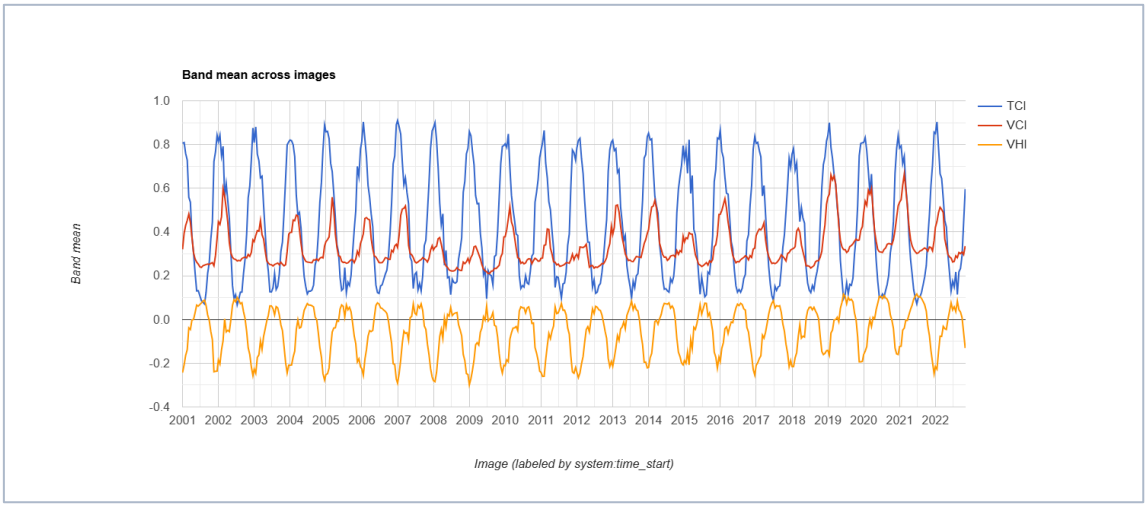

Figure 11. Time-series variations of TCI, VCI, and VHI in Khuzestan Province (2000–2023)

3.6. Seasonal Patterns

Across the 23-year period, VCI and VHI consistently exhibit seasonal cycles. Peaks generally occur in winter and early spring (January–March), indicating periods of higher moisture availability and favorable temperatures for vegetation growth. TCI tends to remain relatively high during these months, reflecting optimal thermal conditions. In contrast, the summer months (June–August) typically show declines in VCI and VHI, reflecting drought stress and the impact of elevated temperatures on vegetation. The combined evaluation of VCI and TCI illustrates that even moderate moisture conditions may lead to reduced vegetation health when thermal stress is significant.

3.7. Interannual Variability

The dataset shows marked year-to-year fluctuations in all three indices. Some years, such as 2001, 2005, 2009, 2015, and 2019, exhibit pronounced negative VHI values, corresponding to periods of severe drought. During these years, both VCI and TCI are reduced, highlighting the compounded effect of water scarcity and thermal stress. Other years, including 2002, 2006, 2016, and 2022, display relatively stable indices with smaller seasonal fluctuations, suggesting favorable climatic conditions and minimal vegetation stress.

3.8. Long-Term Trends

Over the 23-year period, subtle long-term trends are observable. While seasonal patterns remain consistent, peak values of VCI and VHI vary across decades, reflecting interannual climate variability. Periods with higher VHI peaks generally correspond to wetter or cooler years, whereas lower peaks correspond to hotter and drier years. These trends underscore the importance of long-term monitoring for detecting gradual changes in vegetation health and climatic stressors.

3.9. Implications for Drought Monitoring

Analysis of TCI, VCI, and VHI over this extended period highlights their utility for assessing both seasonal and extreme drought events. The integrated evaluation of thermal and moisture conditions allows for a more precise assessment of vegetation stress than any single index alone.

This information is critical for agricultural planning, water resource management, and the development of early warning systems for drought mitigation.

In summary, the 2000–202۳ dataset demonstrates the strong interplay between climatic factors and vegetation health, reinforcing the value of continuous monitoring using VCI, TCI, and VHI for ecological and agricultural management.

3.10. Long-Term Groundwater Storage Changes in Khuzestan Province (2002–2017)

In this study, the long-term trends of groundwater storage in Khuzestan Province were analyzed using GRACE satellite data (Release 06 Version 04) processed through GEE. GRACE delivers monthly terrestrial water storage (TWS) anomalies in equivalent water thickness (EWT), capturing integrated variations in groundwater, soil moisture, surface water, and snow.

The datasets were independently processed by three leading centers: the Center for Space Research (CSR, University of Texas), GeoForschungsZentrum (GFZ, Potsdam), and JPL. To minimize model-specific uncertainties, the ensemble mean of the three solutions was used for spatiotemporal analysis. Additionally, individual datasets from CSR, GFZ, and JPL were analyzed separately to assess inter-model consistency and quantify differences (Figure 12).

The analyzed period spans April 2002 to January 2017, covering the operational lifetime of the original GRACE mission. Accordingly, groundwater storage trends were evaluated for this period, while meteorological drought indices, such as SPI, were examined over longer periods (up to 2025) based on available precipitation records.

The ensemble mean time series (Figure 13) reveals a clear long-term decline in total water storage across Khuzestan. Average TWS anomalies decreased from approximately +7 cm in early 2002 to –15 to –20 cm by 2017, corresponding to a net groundwater loss of ~20–25 cm in equivalent water thickness or roughly 15–20 km³ at the provincial scale.

Temporal variability highlights several periods of sharp depletion, particularly during 2008–2009, 2011–2012, and 2015–2016, which coincide with severe drought episodes identified by SPI, VCI, TCI, and VHI indices. These declines were primarily driven by precipitation deficits, elevated land surface temperatures, and unsustainable groundwater withdrawals for irrigation.

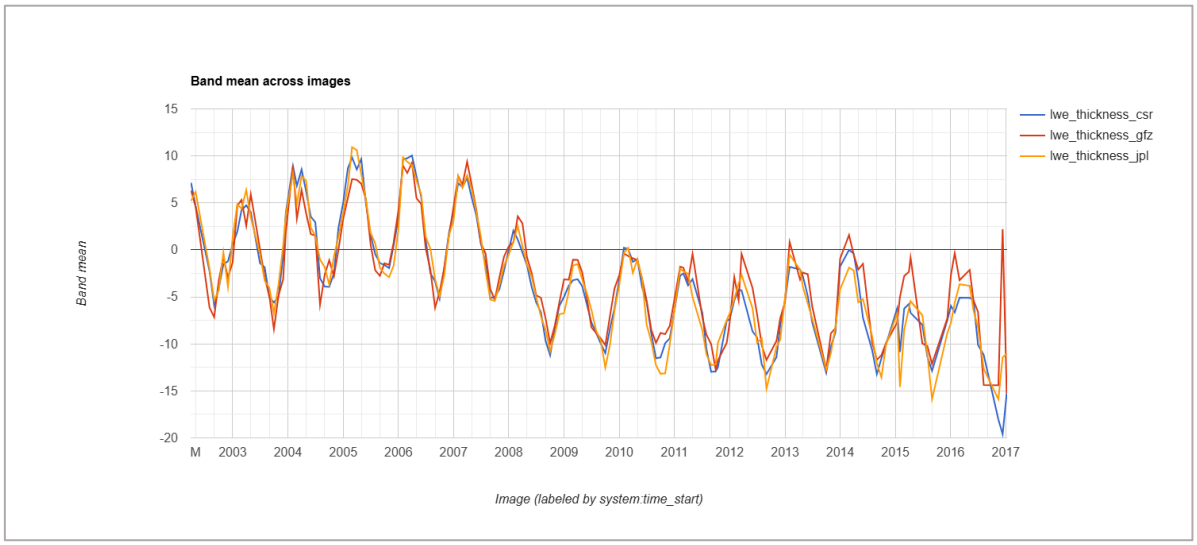

Figure 12. Monthly Terrestrial Water Storage Anomalies in Khuzestan Province from GRACE (2002–2017). Data from CSR, GFZ, and JPL centers are shown along with the three-center ensemble mean.

Comparison among the three GRACE solutions (Figure 13) shows strong agreement in temporal trends, with minor amplitude differences (typically ±2 cm) reflecting variations in processing and post-filtering methods. This consistency reinforces confidence in the observed long-term depletion patterns.

From a spatial perspective, central and eastern Khuzestan experienced the largest declines in groundwater storage, likely due to intensive agricultural activities and limited natural aquifer recharge. In contrast, southern and southwestern regions, particularly the Karun and Karkheh basins, exhibited relatively stable storage, supported by surface water inflows and high-permeability alluvial deposits.

Furthermore, periods of negative TWS anomalies correspond closely with declines in vegetation indices (VCI, VHI), indicating that groundwater depletion not only reflects hydrological stress but also directly impacts vegetation health and ecosystem stability.

In conclusion, both the ensemble mean and individual GRACE datasets confirm a persistent, regionally heterogeneous depletion of groundwater storage in Khuzestan during 2002–2017. These results underscore the combined effects of recurrent droughts, excessive groundwater extraction for agriculture, and insufficient aquifer recharge management, highlighting the urgent need for integrated water resource management in the province.

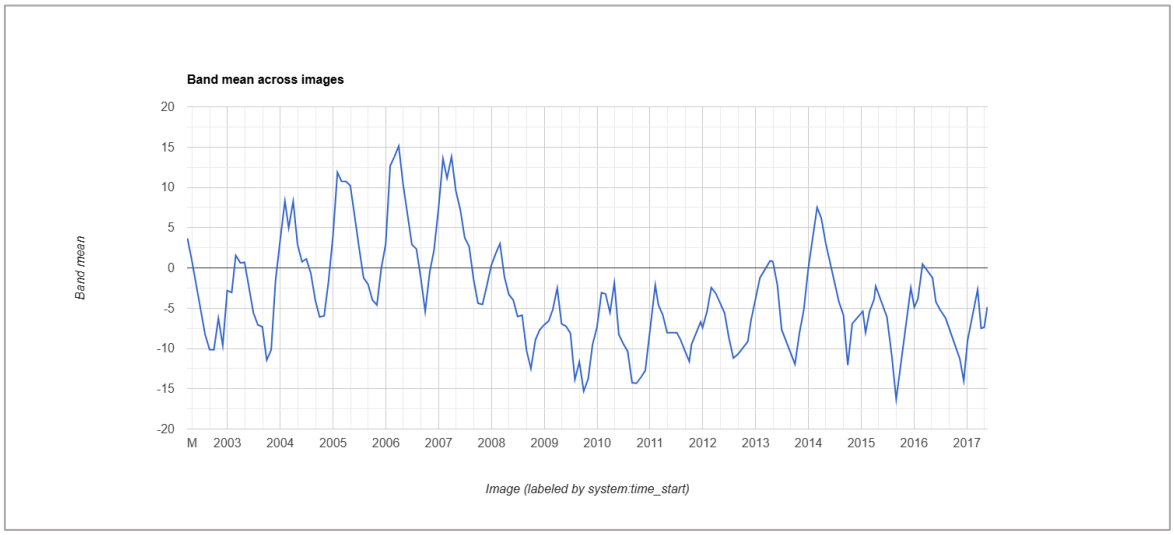

Figure 13. Comparison of GRACE TWS Anomalies among CSR, GFZ, and JPL solutions, highlighting inter-model variability and consistency.

3.11. Surface and Subsurface Soil Moisture Estimation Using SMAP Sensor Data

In this study, the long-term trends of surface soil moisture (SSM) and subsurface soil moisture (SUSM) in Khuzestan Province were analyzed using SMAP satellite data (L3 NASA_USDA/HSL/SMAP_soil_moisture product) processed in GEE. SMAP data are provided every three days, covering the period from January 2015 to January 2020, which represents the full dataset available for analysis. Surface (0–5 cm topsoil) and subsurface (0–30 cm) soil moisture are expressed as volumetric water content (m^3/m^3) and are influenced by environmental factors such as precipitation, evapotranspiration, irrigation, and vegetation cover.

To reduce uncertainties, data were processed using standard SMAP algorithms, and active,

passive, and combined products were compared. Group-averaged time series revealed long-term soil moisture trends, and drought and vegetation indices, including SPI, VCI, TCI, and VHI, were extracted and synchronized with soil moisture variations to assess the effects of soil moisture depletion on ecosystem condition and vegetation health.

The results indicated that the average surface soil moisture (SSM) decreased from approximately 0.28 m^3/m^3 at the beginning of 2015 to 0.20–0.22 m^3/m^3 in 2020, corresponding to an approximate reduction of 5–7 cm in the water thickness of the topsoil layer (Figure 14).

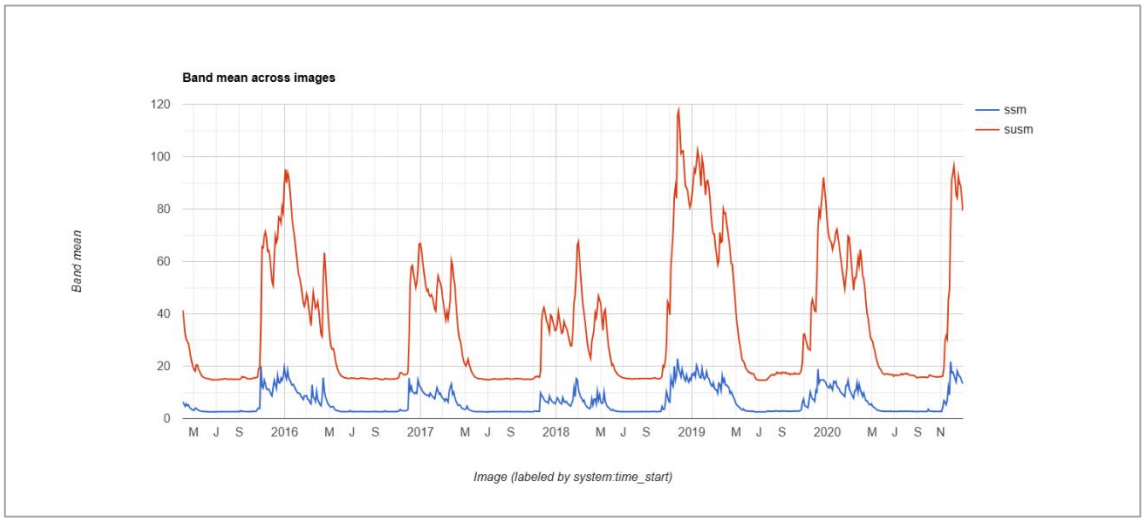

Figure 14. Time series of average surface soil moisture in Khuzestan province from 2015 to 2020

Significant declines in soil moisture during 2015–2016 and 2018–2019 coincided with severe drought periods identified by the SPI. This reduction in soil moisture had a direct impact on vegetation health, as the VCI and VHI indices declined simultaneously with soil moisture, exerting considerable pressure on the ecosystem, whereas the TCI effect was relatively limited and less pronounced (Figure 15).

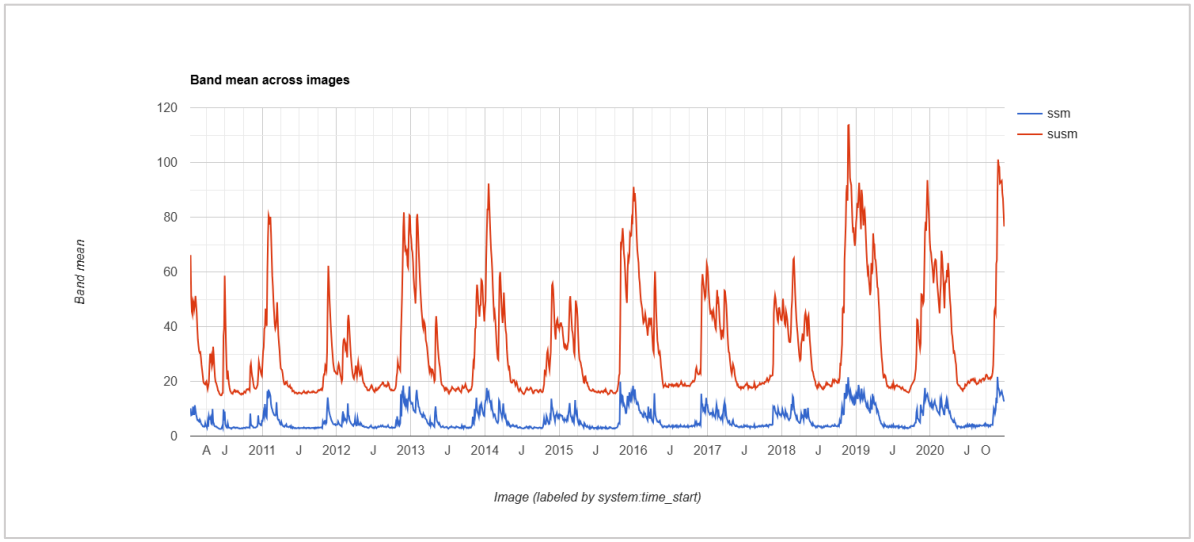

Figure 15. Time series of average subsurface soil moisture in Khuzestan province from 2015 to 2020

Comparisons among different SMAP retrieval methods showed high agreement in temporal trends, with minor discrepancies of ±0.01–0.02 m^3/m^3 due to algorithmic uncertainties and soil texture characteristics, reinforcing confidence in the long-term soil drying pattern.

Overall, this study demonstrates that a persistent and spatially heterogeneous decline in surface and subsurface soil moisture occurred in Khuzestan Province from 2015 to 2020, directly impacting vegetation health and drought indices. These findings highlight the need for integrated soil and water management and indicate that simultaneous monitoring of soil moisture and vegetation indices is the most effective tool for sustainable management of agricultural ecosystems and water resources.

3.12. Validation of Vegetation and Drought Indices

To evaluate the reliability and interrelationships of the computed indices (SPI, VCI, TCI, and VHI) in Khuzestan Province during 2000–2023, Pearson correlation coefficients were calculated. The results are presented in Table 3.

Table 1. Pearson Correlation Coefficients among SPI, VCI, TCI, and VHI (2000–2023)

Index Pair	Pearson r	Interpretation
TCI–SPI	−0.11	Very weak negative correlation; minimal linear dependence between temperature-induced stress and precipitation variability.
VCI–SPI	0.259	Weak positive correlation; vegetation health partially responds to precipitation, influenced by irrigation, soil properties, and local microclimate.
VCI–TCI	−0.004	Near-zero correlation; vegetation vigor is largely independent of temperature stress.
VHI–SPI	0.278	Weak positive correlation; the integrated VHI shows modest sensitivity to precipitation variability.
VHI–TCI	−0.20	Weak negative correlation; thermal stress slightly reduces overall vegetation health.
VHI–VCI	0.979	Very strong positive correlation; VHI is predominantly determined by vegetation condition, with TCI having secondary influence.

The correlation analysis indicates that VHI effectively captures vegetation dynamics and is primarily driven by VCI, as reflected in the very strong positive correlation (r = 0.979). TCI has a minor influence, evidenced by its weak negative correlation with VHI (r = –0.20), suggesting that thermal stress plays a secondary role. SPI exhibits weak correlations with both VCI and VHI (r = 0.259 and 0.278, respectively), implying that precipitation alone does not fully explain vegetation health. These weak correlations may result from lagged vegetation response to rainfall, irrigation practices, and spatial heterogeneity in soil and microclimatic conditions. Overall, these results highlight the importance of considering both vegetation and thermal indices alongside precipitation data when assessing ecosystem health and drought impacts.

4. Discussion

The findings demonstrate that VHI is a robust indicator for capturing vegetation dynamics in Khuzestan, primarily driven by the vegetation condition VCI. The secondary role of TCI, evidenced by its weak negative correlation with VHI, suggests that while thermal stress impacts the ecosystem, it is not the dominant factor compared to moisture availability. The observed weak correlation between SPI and vegetation indices (VCI/VHI) indicates a "lag effect" or a decoupling between immediate precipitation and plant response. This phenomenon is likely

exacerbated by extensive irrigation practices in the southern parts of the province, which buffer vegetation from short-term rainfall deficits. Such complexities highlight the necessity of integrating multiple indices to accurately assess ecosystem health in semi-arid environments.

The weak SPI–VCI relationship observed in this study is consistent with previous research in Iran (Hashemzadeh Ghalhari *et al*., 2022; Barideh & Nasimi, 2025), which identified soil heterogeneity and anthropogenic water management as key factors influencing vegetation resilience. Furthermore, the superiority of a multi-index approach (SPI, VCI, TCI, and VHI) over single-indicator monitoring aligns with the results of Nabizada and Köylü (2025), who emphasized the importance of capturing both moisture and thermal stress simultaneously.

Overall, these results confirm that relying solely on precipitation data (SPI) may lead to an underestimation of drought impacts in Khuzestan. An integrated monitoring framework provides a more comprehensive understanding of the spatiotemporal dynamics of environmental stress, offering a reliable basis for regional water resource management and agricultural planning.

5. Conclusion

This study provides a comprehensive assessment of long-term precipitation variability, vegetation health, and hydrological conditions in Khuzestan Province from 2000 to 2023 using remote-sensing and satellite-derived datasets. The SPI revealed significant seasonal and interannual variability, with dry conditions dominating summer months and occasional extreme wet events in December 2000 and December 2001. Spatial differences in SPI, with higher values in central and eastern regions and drier conditions in western areas, likely reflect variations in precipitation patterns, topography, and water availability.

Vegetation dynamics, assessed via the VCI, TCI, and VHI, exhibited clear seasonal cycles. Peak vegetation health occurred in winter and early spring, while summer declines corresponded to combined moisture and thermal stress. Higher VHI values in southern areas are likely associated with irrigation practices, deeper groundwater access, and soil properties conducive to vegetation growth, whereas central-northern regions experienced recurrent moisture deficits and heat stress. Temporal trends indicate slight recent improvements in vegetation health, although severe drought episodes (e.g., 2008–2009, 2014–2016, 2021–2022) caused notable stress. Correlation analysis confirmed that VHI is predominantly driven by vegetation condition, with SPI and TCI exerting secondary influences. These patterns are consistent with findings from other studies in arid and semi-arid regions (Siasar *et al*., 2025; Javan *et al*., 2025; Eshaghi & Kamkar, 2025; Nabizada *et al*., 2025).

Hydrological analyses using GRACE and SMAP highlighted long-term declines in terrestrial water storage and soil moisture from 2002 to 2017, particularly in central and eastern Khuzestan, reflecting unsustainable groundwater extraction and recurring droughts. Reductions in soil moisture corresponded closely to declines in vegetation indices, demonstrating the tight coupling between water availability and ecosystem health. Regional heterogeneity in vegetation response is influenced by agricultural intensity, crop type, soil texture, and irrigation infrastructure.

The integrated use of SPI, VCI, TCI, and VHI over 2000–2023 demonstrates the value of combining precipitation, vegetation, and hydrological indicators for effective drought monitoring and ecosystem assessment. These results emphasize the need for sustainable water management, targeted agricultural planning, and early warning systems.

Based on the observed spatiotemporal dynamics of drought in Khuzestan, this study suggests

that a multi-index monitoring framework, primarily centered on VHI, can enhance the precision of early warning systems. The findings indicate that mitigation strategies should be prioritized in the central-northern regions, where moisture deficits were most pronounced. Specifically, adopting drought-tolerant crop varieties and optimizing irrigation schedules based on soil moisture data from SMAP could reduce the vulnerability of the agricultural sector. Furthermore, the integration of satellite-derived hydrological indicators provides a more reliable basis for sustainable groundwater management compared to traditional single-index approaches. These strategies offer a practical roadmap for regional stakeholders to minimize the ecological and socio-economic impacts of recurring drought episodes.

Ethical Statement

This research did not involve any human participants or animals. All datasets used in this study were obtained from open-access and publicly available sources, including NASA (MODIS, GRACE, SMAP) and other global data repositories. The study followed all ethical guidelines for the use and processing of remote sensing and environmental data.

Data Availability Statement

The satellite and climate datasets used in this study are publicly accessible from the following sources:

- MODIS data: https://modis.gsfc.nasa.gov/
- GRACE data: https://grace.jpl.nasa.gov/
- SMAP data: https://smap.jpl.nasa.gov/
- Climate data (SPI): acquired from publicly available meteorological databases and reanalysis datasets. Processed data and analysis codes generated during the current study are available from the corresponding author upon reasonable request.

Authors Contribution

Conceptualization, Amir Khazaei and Fatemeh Sahragard; methodology, Amir Khazaei; software, Amir Khazaei; validation, Fatemeh Sahragard and Elham Yousefi; formal analysis, Amir Khazaei; investigation, Amir Khazaei; resources, Fatemeh Sahragard; data curation, Amir Khazaei; writing—original draft preparation, Amir Khazaei; writing—review and editing, Fatemeh Sahragard and Elham Yousefi; visualization, Amir Khazaei; supervision, Elham Yousefi; project administration, Elham Yousefi. All authors have read and agreed to the published version of the manuscript.

Ethics approval and Consent to participate

The data presented in this study are available on reasonable request from the corresponding author.

Acknowledgments

The authors would like to express their sincere appreciation to Dr. Elham Yousefi for her valuable guidance and scientific support throughout this research.

Competing Interests

This study did not involve human participants or animals. The authors avoided data fabrication, falsification, and plagiarism throughout the research process.

Funding
This research did not receive any specific grant from funding agencies in the public, commercial, or not-for-profit sectors.

Consent for Publication
All authors agree to the publication of this manuscript.

Data Availability
The authors declare no conflict of interest. The funders had no role in the design of the study; in the collection, analyses, or interpretation of data; in the writing of the manuscript; or in the decision to publish the results.

References

AghaKouchak, A., Farahmand, A., Melton, F. S., Teixeira, J., Anderson, M. C., Wardlow, B. D., & Hain, C. R. (2015). Remote sensing of drought: Progress, challenges and opportunities. *Reviews of Geophysics, 53*(2), 452–480.

Akhtari, R., Mahdian, M. H., & Morid, S. (2006). Spatial analysis of drought indices SPI and EDI in Tehran Province. *Iranian Journal of Water Resources Research, 2*(3), 27–38.

Aksoy, S., Gorucu, O., & Sertel, E. (2019). Drought monitoring using MODIS derived indices and Google Earth Engine platform. In *Proceedings of the 2019 8th International Conference on Agro-Geoinformatics (Agro-Geoinformatics)* (pp. 1–6). IEEE.

Alzurqani, S. A., Zurqani, H. A., White, D. J., Bridges, K. A., & Jackson, S. A. (2024). Google Earth Engine application for mapping and monitoring drought patterns and trends: A case study in Arkansas, USA. *Ecological Indicators, 168*, 112759. https://doi.org/10.1016/j.ecolind.2024.112759

Amini, A. S., & Hatamzadeh, V. (2023). Remote sensing indexes assessment for drought monitoring using Sentinel satellite imagery: A case study from Natanz County, Iran. *Asian Journal of Geographical Research, 6*(1), 35–43.

Avazpour, F., & Goodarzi, M. R. (2019). Performance of the Standardized Precipitation Index in drought prediction. In *Proceedings of the 3rd Hydrology Conference of Semi-Arid Regions*.

Bahrami, M., Bazrkar, S., & Zarei, A. R. (2019). Modeling, prediction and trend assessment of drought in Iran using standardized precipitation index. *Journal of Water and Climate Change, 10*(1), 181–196.

Bahrami, M., & Mahmoudi, M. R. (2020). Rainfall modelling using backward generalized estimating equations: A case study for Fasa plain, Iran. *Meteorology and Atmospheric Physics, 132*, 771–779.

Barideh, R., & Nasimi, F. (2025). A novel approach to estimating drought-induced damage in rainfed wheat cultivation using modified drought indices. *Theoretical and Applied Climatology, 156*(10), 511. https://doi.org/10.1007/s00704-025-XXXX

Bayissa, Y., et al. (2018). Comparison of satellite-based rainfall products for drought monitoring. *Remote Sensing, 10*, 652.

Bento, V. A., Gouveia, C. M., DaCamara, C. C., & Trigo, I. F. (2018). A climatological assessment of drought impact on vegetation health index. *Agricultural and Forest Meteorology, 259*, 286–295.

Changnon, S. A., Jr., & Easterling, W. E. (1989). Measuring drought impacts: The Illinois case. *Journal of Water Resources Planning and Management, 25*(1), 27–42.

Dehghan, S., Siarei, N., & Bakhtiari, B. (2017). Evaluation of drought trends in Fars Province using Palmer Drought Severity Index. *Iranian Journal of Irrigation and Drainage, 11*(6), 947–959.

Eshaghi, A., & Kamkar, B. (2025). A remote sensing-based framework for agricultural drought risk monitoring and assessment. *Theoretical and Applied Climatology, 156*(12), 684. https://doi.org/10.1007/s00704-025-XYZ

Funk, C., et al. (2015). The climate hazards infrared precipitation with stations (CHIRPS). *Scientific Data, 2*, 150066.

Ganjavian, H., Rezaei Arefi, M., Peysoozi, T., & Emami, K. (2021). Zoning susceptible areas of landslide using WLC and OWA methods: A case study in Mountain Cliff Khan, Iran. *Sustainable Earth Trends, 1*(2), 35–43. https://doi.org/10.52547/sustainearth.1.2.43

Gidey, E., Dikinya, O., Sebego, E., Segosebe, E., & Zenebe, A. (2018). Analysis of agricultural drought using vegetation health index. *Environmental Systems Research, 7*, 1–18.

Gorelick, N., Hancher, M., Dixon, M., Ilyushchenko, S., Thau, D., & Moore, R. (2017). Google Earth Engine: Planetary-scale geospatial analysis for everyone. *Remote Sensing of Environment, 202*, 18–27. https://doi.org/10.1016/j.rse.2017.06.031

Guttman, N. B. (1994). On the sensitivity of sample L-moments to sample size. *Journal of Climate*, 1026–1029.

Hang, Q., Guo, H., Meng, X., Wang, W., Cao, Y., Liu, R., et al. (2024). Optimizing the vegetation health index for agricultural drought monitoring. *Remote Sensing, 16*(23), 4507.

Heim, R. R., Jr. (2002). A review of twentieth-century drought indices used in the United States. *Bulletin of the American Meteorological Society, 83*(8), 1149–1166.

Huete, A. (2004). *Remote sensing for natural resources management and environmental monitoring*. University of Arizona.

Javed, T., Li, Y., Rashid, S., Li, F., Hu, Q., Feng, H., & Pulatov, B. (2021). Performance and relationship of four drought indices. *Science of the Total Environment, 759*, 143530.

Juntakut, P., Jantakat, Y., & Jantakat, C. (2021). Google Earth Engine for monitoring drought impacts on urban tree. *BUILT Journal, 18*, 41–54.

Karimi, M., Shavedi, K., Raziei, T., & Miryaghoubzadeh, M. H. (2019). Efficiency of vegetation indices in agricultural drought analysis. *Iranian Journal of Remote Sensing & GIS, 11*(4), 29–46.

Khalili, P., Konar, M., & Faramarzi, M. (2024). Modelling impacts of future droughts. *Journal of Hydrology*, 131530.

Khan, R., & Gilani, H. (2021). Global drought monitoring with DSI. *Theoretical and Applied Climatology, 146*, 411–427.

Kheyruri, Y., Sharafati, A., & Neshat, A. (2023). Socioeconomic impacts of drought. *Agricultural Water Management, 289*, 108550.

Kogan, F. N. (2001). Operational space technology for global vegetation assessment. *Bulletin of the American Meteorological Society, 82*(9), 1949–1964.

McKee, T. B., Doesken, N. J., & Kleist, J. (1993). The relationship of drought frequency and duration to time scales. *Proceedings of the 8th Conference on Applied Climatology*, 179–183.

Mirzavand, M., & Bagheri, R. (2020). The water crisis in Iran. *World Water Policy, 6*(1), 89–97.

Murugesan, E., et al. (2025). Drought assessment in India. *Journal of Earth System Science, 134*(1), 40.

Nabizada, M. J., & Köylü, Ü. (2025). Multi-sensor drought monitoring. *Theoretical and Applied Climatology, 156*(4), 1–25.

Nouri, H., et al. (2022). Evaluation of CHIRPS precipitation data. *Environmental Earth Sciences, 81*, 1–15.

Omidvar, K., Nabavizadeh, M., Rousta, I., & Olafsson, H. (2024). Remote sensing-based drought monitoring. *Atmosphere, 15*(10), 1211.

Osmani, S. A., Baik, J., Narimani, R., Kim, J. S., & Jun, C. (2024). Agricultural drought indices interactions. *Agricultural Water Management, 302*, 108952.

Piri, S., & Ansari Ghojghar, M. (2025). Machine learning drought modelling. *Journal of Climate Change Research, 6*(22), 8196.

Qin, Q., et al. (2021). Optical and thermal remote sensing for drought monitoring. *Remote Sensing, 13*, 5092.

Quiring, S. M., & Ganesh, S. (2010). Vegetation Condition Index for drought monitoring. *Agricultural and Forest Meteorology, 150*(3), 330–339.

Rahimi, N., et al. (2025). Climate modelling using ANN. *Journal of Water and Climate Change, 16*(2), 531–546.

Rahnama, S., et al. (2024). Comparison of drought indices. *Atmosfera, 38*.

Raziei, T., et al. (2009). Spatial patterns of precipitation in Iran. *Theoretical and Applied Climatology, 97*, 131–142.

Rousta, I., & Al Shoumik, B. A. (2025). Drought monitoring in arid regions. *Journal of Arid Land, 17*(2), 2528137.

Saemian, P., et al. (2022). Water loss in Iran. *Journal of Hydrology: Regional Studies, 41*, 101095.

Singh, R. P., Roy, S., & Kogan, F. (2003). Vegetation indices from NOAA AVHRR. *International Journal of Remote Sensing, 24*(22), 4393–4402.

Tabari, H., et al. (2013). Trends in drought over Iran. *Natural Hazards, 66*, 825–838.

Taheri Qazvini, A., & Carrion, D. (2023). Drought analysis in Google Earth Engine. *Remote Sensing, 15*(9), 2218.

Vicente-Serrano, S. M., et al. (2010). Multiscalar drought index. *Journal of Climate, 23*, 1696–1718.

Winkler, K., Gessner, U., & Hochschild, V. (2017). Droughts affecting agriculture in Africa. *Remote Sensing, 9*(8), 831.